



HHS Public Access

Author manuscript

Nat Neurosci. Author manuscript; available in PMC 2013 February 01.

Published in final edited form as:

Nat Neurosci. ; 15(8): 1160–1166. doi:10.1038/nn.3164.

Early involvement of prefrontal cortex in visual bottom up attention

Fumi Katsuki and Christos Constantinidis

Department of Neurobiology & Anatomy, Wake Forest University School of Medicine, Winston-Salem, NC, USA

Abstract

Visual attention is guided to stimuli based either on their intrinsic saliency against their background (bottom-up factors) or through willful search of known targets (top-down factors). Posterior parietal cortex is thought to play a critical role in the guidance of visual bottom-up attention, whereas prefrontal cortex is thought to represent top-down factors. Contrary to this established view, we found that when monkeys were tested in a task requiring detection of a salient stimulus defined purely by bottom-up factors and whose identity was unknown prior to the presentation of a visual display, prefrontal neurons represented the salient stimulus no later than those in the posterior parietal cortex. This was true even though visual response latency was shorter in parietal than in prefrontal cortex. These results suggest an early involvement of the prefrontal cortex in the bottom-up guidance of visual attention.

The dorsolateral prefrontal (dlPFC) and posterior parietal cortex (PPC) are two brain areas activated during the processing of visuospatial information and orienting of attention, as evidenced by imaging and neurophysiological experiments^{1,2,3,4,5}. Anatomical studies suggest that the posterior parietal cortex comprises the end stage of the dorsal visual pathway, receiving information from visual areas and transmitting it to the dorsolateral prefrontal cortex^{6,7}. This hierarchical and serial nature of organization is captured in current models of visual processing and attention⁸. Recent physiological studies consistent with the serial view also suggest that bottom-up information about the location of salient stimuli is first represented in the posterior parietal cortex (the lateral intraparietal area) and only later in the prefrontal cortex (the frontal eye fields and dlPFC); top-down information follows the reverse course, being represented first in prefrontal and then in parietal cortex⁹.

Determining the time course of saliency representation presents challenges however, stemming from the inherent presence of top-down and bottom-up factors in a behavioral task and the effect of planning of eye movements, which are intrinsically connected with visual

Users may view, print, copy, download and text and data- mine the content in such documents, for the purposes of academic research, subject always to the full Conditions of use: http://www.nature.com/authors/editorial_policies/license.html#terms

Correspondance: Christos Constantinidis, Ph.D. Department of Neurobiology and Anatomy, Wake Forest University School of Medicine, Winston-Salem, NC 27157-1010, USA, Tel: 336-716-7424, Fax: 336-716-4534, cconstan@wfbmc.edu.

AUTHOR CONTRIBUTIONS

F.K. and C.C. designed experiments; F.K. performed experiments; F.K. and C.C. analyzed the data and wrote the paper.

COMPETING FINANCIAL INTERESTS

The authors declare no competing financial interests.

attention circuits^{10,11}. To obtain a physiological estimate of bottom-up representation in the prefrontal and parietal cortex while minimizing the influence of these factors, we recorded neuronal activity in a behavioral task that required subjects to detect a salient stimulus defined solely by bottom-up factors, and to respond with a lever release (not directed to the stimuli) while maintaining fixation. If the posterior parietal cortex plays a general role in the guidance of visual bottom-up attention then, we reasoned, an earlier representation of salient stimulus information would be expected in the activity of parietal neurons, under these circumstances as well. Contrary to this prediction, the results revealed an early involvement of the dorsolateral prefrontal cortex in the representation of salient stimuli.

RESULTS

Two monkeys were trained to perform a task that required them to detect a salient stimulus in a visual display (Fig. 1a) while recordings were performed from the dorsolateral prefrontal and posterior parietal cortex (Fig. 1b, S1). Neither the identity nor the location of the stimulus was known prior to the display appearance; the monkeys were required to recognize the salient (green or red) stimulus by virtue of its color difference from distractor stimuli of equal luminance. The animals indicated correct detection by releasing a lever when a subsequent stimulus appeared at the same location (Fig. 1a). To ensure that the stimuli used in this paradigm “popped out” (and attracted attention automatically), after recordings in this task were completed we retrained the monkeys in a reaction-time version of the task (Fig. 1c) requiring immediate release of the lever once a salient target was detected (and no lever release if it was absent). We found no significant effect of stimulus set size on behavioral response time (regression analysis, slopes of 1.4 and -2.2 ms/item for the two monkeys respectively, $p > 0.5$ in both cases), indicating that stimuli popped out and did not require a serial search of items in the display (Fig. 2).

Time of target discrimination in mean firing rate

A total of 1233 and 479 neurons were recorded during execution of the task of Fig. 1a from the two animals, respectively. We used the same selection criteria in all areas to identify neurons that were responsive to single visual stimuli and displayed significant selectivity for their spatial location (2-way ANOVA, $p < 0.05$). To ensure that any difference in the time of target discrimination between areas was not due purely to a difference in proportion of neurons that were color selective, we initially excluded neurons with significant color selectivity from analysis. We then compared responses to arrays with the salient stimulus appearing in and out of their receptive fields, as defined by the responses to single color stimuli presented at trials randomly interleaved with the array presentations (although this comparison was not a criterion for selection). A total of 278 neurons were analyzed in this fashion in dlPFC, 187 neurons in the lateral intraparietal area (LIP), and 71 neurons in area 7a. In agreement with prior studies^{9,12,13}, many of the neurons responding to single stimuli were selective for salient stimuli of either color (Fig. S2). The time course of neuronal activity that represented the salient stimulus was investigated by comparing the discharge rate elicited by arrays with the target of either color appearing in the receptive field (RF), vs. arrays with distractors in the receptive field. We computed the time at which averaged population discharge rate for the salient stimulus became significantly higher than that of

distractors (time of target discrimination, black arrows in Fig. 3), and used bootstrap methods to determine the variance of this estimate and the statistical significance of differences between areas. Times of target discriminations were 125 ms (s.d.=7 ms) for dlPFC, 125 ms (s.d.=15 ms) for LIP, and 152 ms (s.d.=16 ms) for area 7a neurons. Using a permutation test with equal sample sizes we found no significant difference between dlPFC and LIP times of target discrimination ($p>0.5$) but faster target discrimination in dlPFC than area 7a ($p<0.05$). Alternative measures of target estimation time also confirmed this early involvement of dlPFC, and in the two monkeys separately (Fig. S3a,b). Including neurons with color selectivity in this analysis (Fig. S4) only decreased the relative time of target discrimination in dlPFC (113 ms) compared to LIP (125 ms). Despite this early target discrimination observed in the dlPFC, visual response latencies to stimuli were shorter in the parietal than the prefrontal areas. Population latency values, defined as the times of the earliest visual responses in the population PSTH to arrays with the target in the receptive field (gray arrows in Fig. 3) were 52 ms (s.d.=5 ms) in dlPFC, 42 ms (s.d.=10 ms) in LIP, and 49 ms (s.d.=8 ms) in area 7a.

We sought to verify these findings on a neuron-by-neuron basis as well (Fig. S5), identifying latency and time of target discrimination separately for each neuron with the same criteria described above (although for some neurons insufficient number of spikes were available to perform this analysis). The neuron-by-neuron analysis showed that average neuronal visual response latency was significantly longer (t-test, $p<0.05$) in dlPFC (mean=107, s.d.=82 ms) than in LIP (mean=93, s.d.=70 ms), whereas the average time of target discrimination (mean=182, s.d.=95 ms in dlPFC vs. mean=192, and s.d.=86 ms in LIP) was not significantly different between areas (t-test, $p>0.3$). The results of the neuron-by-neuron basis analysis confirmed that the target discrimination in prefrontal cortex occurred no later than the parietal cortex, suggesting that the location of the salient stimulus was computed independently within the prefrontal cortex, rather than being transmitted in a serial fashion from the parietal cortex. The result also implied that the available processing time between visual response latency and time of target discrimination is shorter in dlPFC than in LIP. Indeed, when we examined the processing time on a neuron-by-neuron basis, we found it to be significantly shorter (t-test, $p<0.05$) in dlPFC (75 ms) than LIP (99 ms).

To ensure that this early representation of a salient stimulus by the prefrontal cortex was not somehow the result of random variation of perceptual time across sessions in which the prefrontal and posterior parietal data were collected, we also analyzed recordings that were performed simultaneously from the prefrontal and the parietal cortex. In these sessions, 71 dlPFC and 61 LIP neurons were recorded simultaneously, as were 48 dlPFC neurons and 23 area 7a neurons. The times of target discrimination in this sample were again not significantly different between dlPFC and LIP (permutation test, $p>0.05$) and if anything, slightly earlier in dlPFC (121 vs. 128 ms in dlPFC and LIP, respectively); visual response latencies were 45 ms for dlPFC and 44 ms for LIP. The time of target discrimination was significantly earlier for dlPFC than area 7a in this sample, as well (permutation test, $p<0.05$).

Anatomical and functional evidence suggests that the prefrontal cortex itself may be organized in a hierarchical fashion across the rostro-caudal axis^{14,15}. We therefore wished to determine whether an early time of target discrimination was present only in the posterior

part of the prefrontal cortex. For this analysis, we divided recording sites in an anterior and a posterior half for each monkey, and repeated the estimate of visual response latency and time of target discrimination (Fig. S6). The population visual response latency for the posterior prefrontal cortex was indeed very similar to that of LIP (41 vs. 42 ms), though considerably longer for the anterior aspect of the dIPFC (55 ms). However, the time of target discrimination in the anterior dIPFC (129 ms) was still not significantly different (permutation test, $p > 0.3$) than that of LIP (125 ms). In fact, the difference between visual response latency and time of target discrimination was the shortest in the anterior dIPFC (74 ms) compared to the posterior dIPFC (87 ms), and LIP (99 ms). The results argue against a serial transmission of the saliency signal from LIP first to the posterior dIPFC and then to the anterior dIPFC.

Target discriminability

The finding of an early prefrontal activation in response to the salient stimulus also translated into an early target discrimination, from a signal detection standpoint. A time-resolved receiver operating characteristic (ROC) analysis comparing responses to a salient stimulus vs. a distractor indicated that the area under the ROC curve, constructed based on average neuronal responses, rose in dIPFC as early as in LIP, and faster than in area 7a (Fig. 4a). To ensure that this average ROC value did not obscure a population of LIP neurons that may be able to detect the salient stimulus faster, we also performed a neuron-by-neuron ROC analysis (Fig. 4b). A bootstrap test was used to estimate the time point when the area under the ROC curve became significantly different than chance. A total of 156 dIPFC neurons, 116 LIP neurons, and 27 area 7a neurons reached significance based on this criterion. No significant difference existed between the dIPFC and LIP distributions (Kolmogorov-Smirnov test, $p > 0.1$); if anything, the LIP distribution trailed dIPFC at early time points between 100–150 ms after stimulus onset. Similar patterns of ROC values were observed in both monkeys (Fig. S3c,d).

Target discrimination based on neuronal responses is essentially a signal detection problem and stronger signals will on average be detected earlier than weaker signals. For this reason, early detection of the target in the prefrontal cortex may merely be an effect of stronger discrimination of the stimuli. We therefore examined the relationship between discriminability (determined as the area under the ROC) and time of target discrimination (Fig. 5). As predicted, the two variables were negatively correlated (PFC: $r = -0.28$, $p < 10^{-4}$; LIP: $r = 0.15$, $p = 0.08$). We then performed an analysis of covariance (ANCOVA) comparing the times of target discrimination between areas, treating the area under the ROC curve as a covariate. When discounting for the effect of strength of discriminability in this way, dIPFC discriminated the target faster than LIP by 6 ms on average, a non-significant difference (intercept comparison, $p > 0.05$). We also analyzed the group of neurons at the top quartile of discrimination values, pooled across both areas. Target discrimination of dIPFC neurons in this sample was 27 ms faster than that of LIP neurons (which had essentially identical mean ROC values of 0.900 and 0.898), a difference at the margin of statistical significance (t-test, $p = 0.048$).

The analysis presented so far was based on neurons with significant visual responses and spatial selectivity for single stimuli. It has been argued, however, that information about salient stimuli may be more subtle, and that an informational theoretical approach examining data from all neurons may be more appropriate⁹. We therefore performed a mutual information analysis on all recorded neurons, with no regard for spatial selectivity – or even overt responses to visual stimuli. Our entire sample of 793 dIPFC neurons, 406 LIP neurons, and 485 area 7a neurons were tested in this way. The mutual information statistic reflects how well one can separate the salient stimulus location from other locations based on the firing rate of a neuron. The number of neurons with significant information in each time bin started rising in dIPFC and LIP with similar time courses (Fig. 4c). This was also illustrated in the cumulative distribution of neurons that reflected significant information at each time point (Fig. 4d) which was not significantly different between areas LIP and dIPFC (Kolmogorov-Smirnov test, $p>0.7$). Similar patterns were observed for the two monkeys (Fig. S3e,f). The results confirm that dIPFC neurons reflect information about the target location no later than posterior parietal ones.

Reaction-time task

It could be argued that the time of target discrimination reflected in the neuronal activity in our task was not critical for the selection of salient stimuli since the subjects were only tested after the presentation of the stimulus array and an intervening delay period (Fig. 1a). For this reason, we also collected recordings from 561 neurons in a reaction-time version of the task (Fig. 1c). In this task, the monkey was required to release the lever as fast as it detected the salient stimulus (and to hold if a salient stimulus was not present). Analysis of neuronal recordings revealed that the neuronal target detection in this task were overall faster than in the match-to-sample task (Fig. 6a,b). The average times of target detection were 107 ms for dIPFC, 105 ms for LIP, and 120 ms for 7a, an average of 23 ms difference over the match-to-sample task. The time of target detection remained not-significantly different between dIPFC and LIP (permutation test, $p>0.4$), although the average response latency was again considerably shorter for LIP than dIPFC (47 vs. 60 ms, respectively). No earlier target detection was observed for LIP, when we aligned responses to the lever release, and comparing neurons recorded simultaneously (Fig. 6c,d). ROC and mutual information analysis confirmed that target discriminability and information did not appear earlier in LIP than dIPFC (Kolmogorov-Smirnov test, $p>0.6$ for ROC comparison in Fig. S7b, $p>0.3$ for mutual information comparison in Fig. S7d).

To gain insight on the nature of salient stimulus representation, we also examined error trials in which the target was present but the monkey missed it and those in which the target was absent, yet the monkey falsely reported its presence (Fig. S8). Comparing firing rates of neurons for which both misses and false alarms were available, we observed a similar pattern between areas. Average firing rate in the time interval of 0–300 ms after the stimulus onset was lower in misses than in hits for both dIPFC (26.0 vs. 29.4 spikes/s) and LIP (18.5 vs. 20.3 spikes/s). Firing rate was greater in false alarm than in correct rejections (22.3 vs. 21.8 spikes/s in dIPFC, and 17.9 vs. 15.6 spikes/s in LIP). The time course of the difference in firing rate in correct and error trials had little predictive power over the time course of target discrimination, as the two were not significantly correlated in either area ($r=0.2$ in

dIPFC, $r=0.02$ in LIP, $p>0.2$ in both cases). This result indicates that firing rate differences in correct and error trials were not tightly tied with the time of target discrimination in either area and the time of target discrimination could not be accounted for by behavioral choice. We did note however that the difference in response between target and distractors (Fig. S8c) diminished greatly in error trials for LIP (-87%), and less so for dIPFC (-51%).

Difficulty and display size

It is conceivable that the lack of a temporal advantage by the posterior parietal cortex only applies to unambiguous, highly salient stimuli; the parietal cortex may still be critical in orienting attention to less salient stimuli. We examined this possibility by varying the distractor color so as to render the target stimulus more difficult to detect. In an initial set of experiments we identified four levels of chromatic contrast over which performance declined in an approximately linear fashion (Fig. S9a). We then analyzed neuronal activity recorded from 58 dIPFC, 55 LIP and 25 area 7a neurons during presentation of these displays in the context of the match-to-sample task. In agreement to previous studies¹⁶, responses to arrays with target stimuli among more similar distractors were generally weaker and the time of target discrimination occurred later (Fig. 7a). However, we did not observe a significant advantage of the posterior parietal cortex over dIPFC (Fig. 7b), for any level of difficulty (permutation test, $p>0.1$ for all comparisons), or based on ROC and mutual information analysis (Fig. 8). This result was consistent with an early involvement of dIPFC in the representation of target stimuli even when they were more difficult to discriminate.

It is also possible that systematic differences in receptive field size between the prefrontal and posterior parietal neurons we sampled influence the processing time for displays of different size. To determine whether the early activation of the prefrontal cortex generalizes across display size, we trained the monkeys to perform the reaction-time version of the task, using a denser array of 3° stimuli, spaced 7° apart from each other (instead of 15° , for the previous experiments). A total of 140 and 399 neurons were recorded from the two monkeys respectively, 242 from dIPFC and 297 from LIP. Difference in firing rate for the best and worst location in this dense array was lower overall (Fig. S10), however the timing of mutual information for stimulus location indicated no significant difference between the distributions of dIPFC and LIP neurons for this stimulus set, either (Kolmogorov-Smirnov test, $p>0.9$).

DISCUSSION

Early psychophysical experiments showed that visual attention is guided automatically to stimuli that stand from their background by virtue of their inherent saliency, a process referred to as “bottom-up” attention^{17,18}. Attention may also be allocated willfully, e.g. when actively scanning the visual field for a known target, known as “top-down” attention¹⁹. Neurophysiological correlates of selective representation of stimuli that differ from their local background are evident as early as area V1, and with very short latencies²⁰. However, responses in early visual areas are not adequate for guiding attention to the overall most salient stimulus in the field of view, as neurons have access to information over a small

receptive field area^{21,22}. For bottom-up attention to be deployed effectively, information from all feature streams is thought to be represented in a global saliency or priority map^{23,24}. It is now clear that saliency maps are simultaneously present in multiple brain areas²⁵, including areas LIP and 7a in the parietal lobe^{12,26}, the frontal eye fields (FEF)¹³ in the frontal lobe, and the superior colliculus²⁷. Our present results demonstrate early involvement of the dorsolateral prefrontal cortex in visual attention guided by a target stimulus that is defined purely by bottom-up factors and so add dlPFC in this list. Our results also demonstrate that detection of the salient stimulus in these areas proceeds in a parallel, rather than a serial manner, unlike the pattern of visual response latency.

Our finding of early involvement of the prefrontal cortex in bottom-up attention is consistent with some neurophysiological studies that have suggested similar patterns of activation in parietal and frontal areas (LIP and FEF), though these studies did not involve recordings from both areas in the same animals^{28,29}. Recent imaging studies also report robust prefrontal activation in bottom-up visual search³⁰. Finally, anatomical studies show that the pattern of projections between the parietal and prefrontal cortex is parallel (originating from and terminating to the same layers in both directions) rather than strictly serial^{7,31}, as would have been predicted by a hierarchical relationship between the parietal and prefrontal cortex²⁵.

On the other hand, our conclusions stand in contrast with a previous neurophysiological study finding faster LIP recruitment during detection of pop-out stimuli⁹. The study reported comparable mean time of target discrimination in LIP to the 105 ms we report here for the reaction time task (based on firing rate), but much slower for FEF (>150 ms) and dlPFC. There are some critical differences between the studies, including the absence of a saccade requirement in our task, which preferentially activates LIP neurons³², and the use of stimuli appearing in peripheral vision in our task (where most ecologically important stimuli are likely to appear first) as opposed to perifoveal stimuli within 4° of the center of vision. The time of stimulus discrimination also appears to be considerably sensitive on stimulus parameters. Mean target discrimination times as early as 50–70 ms have been reported recently in the literature for area LIP^{33,34}. Experiments relying on much larger stimuli in a match-to-sample task also resulted in faster discrimination times in area 7a¹² than those we report here for the same area.

Although we have emphasized that the target was defined by bottom-up factors in our task, top-down factors undoubtedly were present as well; the monkey was required to interpret the color of the stimuli in the display and conditionally release a lever. The earlier involvement of the prefrontal cortex in our study seems unlikely however to be driven purely by top-down factors since equivalent factors were present in the prior study⁹ (in fact, it is arguable whether that task relied on bottom-up factors, since the animals were explicitly cued about the sought out target in each trial). We did see that the absolute time of target discrimination in neuronal activity decreased considerably when the same animals were required to perform a reaction time task, compared to the match-to-sample task. A corresponding change in the time of target discrimination has previously been observed in animals trained to search for a specific stimulus feature³⁵ (faster discrimination) or not required to perform a task at all³⁶ (slower discrimination). There is little doubt, therefore, that task demands can influence the

time of target representation in neuronal activity, and comparison of the absolute time of target discrimination across experiments may be of little value. We should also point out that a similar time course of target representation does not necessarily imply that the two brain regions play identical roles. Our current results do provide evidence for early involvement of the prefrontal cortex in the guidance of visual attention by bottom up factors that cannot be accounted for by the posterior parietal cortex.

METHODS

Two male, rhesus monkeys (*Macaca mulatta*) weighing 5–8 kg were used in this study. All surgical and animal use procedures were conducted with approval from Institutional Animal Care and Use Committee of the Wake Forest University according to National Institutes of Health guidelines.

Behavioral tasks

The monkeys sat in front of a computer monitor positioned 60 cm away with their head fixed in a dark room. While the monkeys were maintaining their gaze on a white target of 0.2° in size located at the center of the screen, visual stimuli were presented. Eye position was sampled at 240 Hz, digitized, and recorded using an infrared eye position tracking system (model RK-716; ISCAN, Burlington, MA). If the animals broke fixation exceeding a 2° window, the trial was immediately terminated. The monkeys were rewarded with fruit juice upon correct completion of a trial. The visual stimulus presentation, online monitoring of eye position, and synchronization of stimuli with neurophysiological data were controlled by in-house software³⁷, implemented in MATLAB (Mathworks, Natick, MA), using the Psychophysics Toolbox³⁸.

Monkeys were tested with the delayed match-to-sample task which required them to locate a salient stimulus among distractors and to release a lever when a subsequent stimulus appeared at the location of the salient stimulus (Fig. 1a). The trial started with the animals pulling a behavioral lever and fixating at the center of the monitor. The cue was displayed at one of nine locations, with or without distractor stimuli. The cue was rendered salient due to its difference in color from 8 distractors arranged along a 3×3 grid of 15° separation between adjacent stimuli (diagonal elements appeared at an eccentricity of 21°). Stimuli consisted of green or red squares of 1.5° in size. In some sessions the salient stimulus appeared at any of 4 possible locations (either the cardinal or diagonal positions in the array). The location of the stimulus was randomized from trial to trial, and stimulus arrays with cue and distractors of either green or red color were randomly interleaved with equal probability. The monkeys therefore were not able to predict either the location or the identity of the salient stimulus. The cue was displayed for 0.5 s followed by a delay period of 1.0 s. Then, a pseudorandom sequence of 0–2 non-match stimuli was presented, each lasting 0.5 s and separated by delay periods of 0.5 s. The sequence ended with a match stimulus appearing at the same location as the cue. The animals were trained to hold the lever until a match presentation (0.5 s) and to release the lever within 0.5 s after the match stimulus disappeared in order to receive a liquid reward. Release of the lever at any other time during the trial was considered as an error, and the trial was immediately aborted.

A variation of the basic task (referred to as the “difficult-discrimination” task in the main text) involved the same target stimuli (red/green) appearing among distractors of varying similarity. Four levels of difficulty were used involving a) same distractor stimuli (green/red) as those used in the standard task, b) distractor stimuli identical to the target, rendering the presentation a “catch trial” rewarded randomly, and c–d) two intermediate levels of chromatic difference. Psychophysical performance decreased monotonically for targets of either color (Fig. S9).

To assess the animal’s speed in detecting the salient stimulus, a reaction-time version of the task was also used (Fig. 1c). In this task, the monkey was required to release the lever as quickly as possible when a target was present in the display and keep holding the lever if there was no target. If the monkey continued to hold the key after 0.8 s and a salient stimulus was present, then the trial was aborted; if the salient stimulus was not present then the monkey was rewarded. In this task, the duration of the fixation period also varied randomly so as to make it impossible to time the lever release. A denser stimulus array with 3° size stimuli, spaced 7° apart of each other was also used in the reaction-time task. Displays with variable number of distractor stimuli (0, 2, 4, or 8) were also used in some sessions, to determine the effect of set size on reaction time.

Surgery and neurophysiology

After the animals were trained, they were prepared for neurophysiological recordings. Two 20 mm diameter recording cylinders were implanted over the prefrontal and parietal cortex of the same hemisphere followed by a craniotomy. Extracellular recordings were performed using arrays of 2–8 microelectrodes in each cylinder. We used either glass-coated, tungsten electrodes of 250 μm diameter, with an impedance of 1 $\text{M}\Omega$ at 1 kHz (Alpha-Omega Engineering, Nazareth, Israel) or epoxy-coated tungsten electrodes with a diameter of 125 μm and an impedance of 4 $\text{M}\Omega$ measured at 1 KHz (FHC Bowdoin, ME). Electrodes were positioned through a grid system and advanced into the cortex with a microdrive system (EPS drive, Alpha-Omega Engineering, Nazareth, Israel). The electrical signal obtained from each electrode was amplified, band-pass filtered between 500 and 8 kHz, and recorded with a modular data acquisition system (APM system, FHC, Bowdoin, ME). Waveforms that reached a user-defined threshold were sampled at 25 μs resolution, digitized, and stored for off-line analysis.

The anatomical location of electrode penetration was determined based on MR imaging of the brain after implantation of the recording cylinders. Prefrontal data were collected from areas 8a and 46 including both banks of the principal sulcus, the area between the principal and the arcuate sulcus, and the superior convexity of the lateral prefrontal cortex. Posterior parietal data were collected from area 7a at the crown of the gyrus posterior to the intraparietal sulcus and the lateral intraparietal area (LIP) in the lateral bank of the intraparietal sulcus, at depths >3 mm from the surface of the cortex. These parietal areas are directly interconnected with the prefrontal cortex³⁹.

Data analysis

Spike waveforms were sorted into separate units using an automated cluster analysis method based on the KlustaKwik algorithm⁴⁰, which applied principal component analysis of the waveforms. We then identified units with significant elevation of firing rate during the 0.5 s of visual stimulus presentation compared to 0.5 s interval of fixation (paired t-test, $p < 0.05$). Only the data during the cue period from correct trials were used for the analysis. The spatial tuning of visually responsive neurons was assessed by comparing the discharge rates during the presentation of single stimuli of either color at the nine grid locations. Neurons with significant main effect of stimulus location (2-way ANOVA; $p < 0.05$) but no significant main effect of color (2-way ANOVA; $p > 0.05$) were included in analysis. An additional analysis using all neurons exhibiting significant location selectivity with or without color selectivity was also performed (Fig. S4). For the reaction-time task with a denser stimulus array, all neurons with significant visual response were used (Fig. S10).

Population peri-stimulus time histograms (PSTHs) were constructed averaging responses of all neurons from each area, pooling data from salient stimuli of both colors. Average population visual response latency in each area was determined based on the population responses, as the first of 10 consecutive 10 ms windows stepped by 1 ms that were significantly higher (paired t-test, $p < 0.05$) than the baseline firing rate⁴¹. We relied on an analogous procedure to determine the time of target discrimination: we identified the time point of the first of 10 consecutive 10 ms bin windows stepped by 1 ms, for which population responses to a salient stimulus inside the receptive field were significantly higher than responses to distractors (paired t-test, $p < 0.05$). Differences between areas were tested by using a bootstrap test⁴² in which population PSTHs were computed by randomly sampling neurons regardless of area, calculating response latencies or target discrimination times, and repeating the procedure 1000 times. The significance value of the observed differences was determined based on the empirical distribution of latencies of the randomized tests. An alternative method of latency estimation (Fig. S3a,b) was based on determining the inflection point of the cumulative sum of neuronal responses⁴³.

We also analyzed trials that resulted in errors in the reaction time version of the task, excluding error trials due to breaks in fixation and blinks. Error trials were categorized into two types: misses in which the target was present but the monkey did not release the lever, and false alarms in which the target was absent but the monkey released the lever. Firing rate of each error type was computed and compared with firing rates of two types of correct trials (Fig. S8). For correct trials, the difference in firing rate between target-present and target-absent trials was computed across time. For error trials, the absolute difference in firing rate between miss and hit trials, as well as between false-alarm and correct rejection trials was calculated separately, and then averaged together. A correlation coefficient was computed between the averaged absolute values of firing rate difference obtained with error trials and the firing rate difference obtained with correct trials in the interval of 0–300 ms after cue onset. To investigate if target discriminability changed in error trials, averaged firing rates over 0–300 ms after cue onset were also calculated for each of the four conditions.

A receiver operating characteristic (ROC) analysis was performed by comparing the distributions of firing rates of a neuron to stimulus arrays with the salient stimulus appearing at the location that elicited the best responses in the receptive field and at its diametric location¹². The area under the ROC curve represents the probability that an ideal observer can discriminate between a salient stimulus and a distractor based on their firing rate in each trial⁴⁴. The analysis was performed in a time-resolved fashion, comparing responses in a 25 ms long moving window, computed in 10 ms steps²⁹. A bootstrap test was also performed to evaluate the significance of the area under the ROC curve. For each neuron, ROC values were obtained based on samples of responses obtained with no regard of whether they were recorded during the presentation of the salient stimulus in the receptive field or opposite to it. Significance was evaluated for the observed ROC value based on the distribution of the randomized ROC values (bootstrap test with 1000 repetitions). For each bin, the observed ROC value was presumed to be significant if the value exceeded 95% of the randomized distribution ($p < 0.05$). The time point when a neuron reached significance was defined as the first of two consecutive bins with significant ROC values.

For the comparison of the relationship between discriminability and time of target discrimination (Fig. 5), the area under the ROC curve was computed over the entire stimulus presentation period (500 ms) for each neuron. The top quartile of ROC values was determined after pooling the values of both areas together and used that as a common criterion for both areas. Neurons that met the criterion were used to compare the time of target discrimination between areas. Analysis of covariance (ANCOVA) was conducted by applying a linear model on the data from two areas given with the time of target discrimination as the dependent variable and target discriminability (the area under the ROC) as a covariate.

A mutual information statistic was calculated to determine how well the salient stimulus location can be discriminated from others, based on the firing rate of a neuron⁴⁵. Mutual information was calculated in non-overlapping 25 ms time windows and values were averaged across neurons in each area. Statistical significance was determined by means of a bootstrap test: data were randomly sampled with no regard of the actual salient stimulus location. The process was repeated 1000 times and the observed mutual information value was compared to this randomized distribution. The time point when each neuron's activity began to significantly represent the target location was defined as the time point when mutual information values became significant for two successive bins (one for the dense stimulus array).

Supplementary Material

Refer to Web version on PubMed Central for supplementary material.

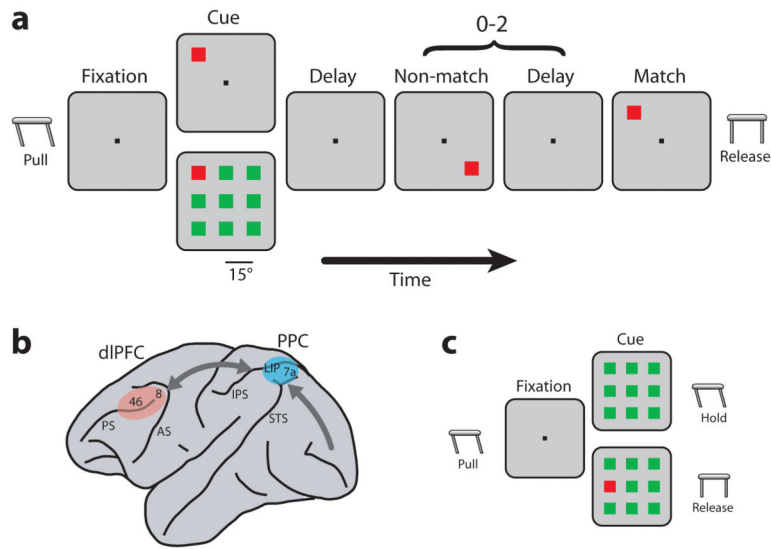
Acknowledgments

Research reported in this paper was supported by the National Eye Institute of the National Institutes of Health under award number R01EY16773, and by the Tab Williams Family Endowment Fund. We wish to thank Kathini Palaninathan, Keith Roberts, and Justin Rawley with help in experiments; Ram Ramachandran, Terry Stanford, and Emilio Salinas for comments.

References

1. Bisley JW, Goldberg ME. Attention, intention, and priority in the parietal lobe. *Annu Rev Neurosci.* 2010; 33:1–21. [PubMed: 20192813]
2. Schall JD. The neural selection and control of saccades by the frontal eye field. *Philos Trans R Soc Lond B Biol Sci.* 2002; 357:1073–1082. [PubMed: 12217175]
3. Noudoost B, Chang MH, Steinmetz NA, Moore T. Top-down control of visual attention. *Curr Opin Neurobiol.* 2010; 20:183–190. [PubMed: 20303256]
4. Connor CE, Egeth HE, Yantis S. Visual attention: bottom-up versus top-down. *Curr Biol.* 2004; 14:R850–852. [PubMed: 15458666]
5. Corbetta M, Shulman GL. Control of goal-directed and stimulus-driven attention in the brain. *Nat Rev Neurosci.* 2002; 3:201–215. [PubMed: 11994752]
6. Ungerleider, LG.; Mishkin, M. *Analysis of Visual Behavior.* Ingle, DJ.; Goodale, MA.; Mansfield, RJW., editors. MIT Press; 1982. p. 549-586.
7. Felleman DJ, Van Essen DC. Distributed hierarchical processing in the primate cerebral cortex. *Cereb Cortex.* 1991; 1:1–47. [PubMed: 1822724]
8. Serre T, Oliva A, Poggio T. A feedforward architecture accounts for rapid categorization. *Proc Natl Acad Sci U S A.* 2007; 104:6424–6429. [PubMed: 17404214]
9. Buschman TJ, Miller EK. Top-down versus bottom-up control of attention in the prefrontal and posterior parietal cortices. *Science.* 2007; 315:1860–1862. [PubMed: 17395832]
10. Kustov AA, Robinson DL. Shared neural control of attentional shifts and eye movements. *Nature.* 1996; 384:74–77. [PubMed: 8900281]
11. Moore T, Fallah M. Control of eye movements and spatial attention. *Proc Natl Acad Sci U S A.* 2001; 98:1273–1276. [PubMed: 11158629]
12. Constantinidis C, Steinmetz MA. Neuronal responses in area 7a to multiple stimulus displays: I. Neurons encode the location of the salient stimulus. *Cereb Cortex.* 2001; 11:581–591. [PubMed: 11415960]
13. Schall JD, Hanes DP. Neural basis of saccade target selection in frontal eye field during visual search. *Nature.* 1993; 366:467–469. [PubMed: 8247155]
14. Preuss TM, Goldman-Rakic PS. Myelo- and cytoarchitecture of the granular frontal cortex and surrounding regions in the strepsirrhine primate Galago and the anthropoid primate Macaca. *J Comp Neurol.* 1991; 310:429–474. [PubMed: 1939732]
15. Badre D, D’Esposito M. Is the rostro-caudal axis of the frontal lobe hierarchical? *Nat Rev Neurosci.* 2009; 10:659–669. [PubMed: 19672274]
16. Sato TR, Watanabe K, Thompson KG, Schall JD. Effect of target-distractor similarity on FEF visual selection in the absence of the target. *Exp Brain Res.* 2003; 151:356–363. Epub 2003 Jun 2012. [PubMed: 12802550]
17. Treisman AM, Gelade G. A feature-integration theory of attention. *Cognit Psychol.* 1980; 12:97–136. [PubMed: 7351125]
18. Wolfe JM. Guided Search 2.0 - a Revised Model of Visual-Search. *Psychon Bull Rev.* 1994; 1:202–238. [PubMed: 24203471]
19. Itti L, Koch C. Computational modelling of visual attention. *Nat Rev Neurosci.* 2001; 2:194–203. [PubMed: 11256080]
20. Knierim JJ, van Essen DC. Neuronal responses to static texture patterns in area V1 of the alert macaque monkey. *J Neurophysiol.* 1992; 67:961–980. [PubMed: 1588394]
21. Hegde J, Felleman DJ. How selective are V1 cells for pop-out stimuli? *J Neurosci.* 2003; 23:9968–9980. [PubMed: 14602810]
22. Burrows BE, Moore T. Influence and limitations of popout in the selection of salient visual stimuli by area V4 neurons. *J Neurosci.* 2009; 29:15169–15177. [PubMed: 19955369]
23. Koch C, Ullman S. Shifts in selective visual attention: towards the underlying neural circuitry. *Human Neurobiology.* 1985; 4:219–227. [PubMed: 3836989]
24. Niebur, E.; Koch, C. *Neural Information Processing Systems.* Touretzky, DS.; Mozer, MC.; Hasselmo, ME., editors. MIT Press; 1996. p. 802-808.

25. Katsuki F, Constantinidis C. Unique and shared roles of the posterior parietal and dorsolateral prefrontal cortex in cognitive functions. *Front Int Neurosci.* 2012; 6:17.
26. Gottlieb JP, Kusunoki M, Goldberg ME. The representation of visual salience in monkey parietal cortex. *Nature.* 1998; 391:481–484. [PubMed: 9461214]
27. McPeck RM, Keller EL. Saccade target selection in the superior colliculus during a visual search task. *J Neurophysiol.* 2002; 88:2019–2034. [PubMed: 12364525]
28. Thomas NW, Pare M. Temporal processing of saccade targets in parietal cortex area LIP during visual search. *J Neurophysiol.* 2007; 97:942–947. [PubMed: 17079346]
29. Thompson KG, Hanes DP, Bichot NP, Schall JD. Perceptual and motor processing stages identified in the activity of macaque frontal eye field neurons during visual search. *J Neurophysiol.* 1996; 76:4040–4055. [PubMed: 8985899]
30. Wardak C, Vanduffel W, Orban GA. Searching for a salient target involves frontal regions. *Cereb Cortex.* 2010; 20:2464–2477. [PubMed: 20100901]
31. Cavada C, Goldman-Rakic PS. Posterior parietal cortex in rhesus monkey: II. Evidence for segregated corticocortical networks linking sensory and limbic areas with the frontal lobe. *J Comp Neurol.* 1989; 287:422–445. [PubMed: 2477406]
32. Constantinidis C. Posterior parietal mechanisms of visual attention. *Rev Neurosci.* 2006; 17:415–427. [PubMed: 17139842]
33. Arcizet F, Mirpour K, Bisley JW. A Pure Salience Response in Posterior Parietal Cortex. *Cereb Cortex.* 2011
34. Premereur E, Vanduffel W, Janssen P. Functional heterogeneity of macaque lateral intraparietal neurons. *J Neurosci.* 2011; 31:12307–12317. [PubMed: 21865473]
35. Bichot NP, Schall JD, Thompson KG. Visual feature selectivity in frontal eye fields induced by experience in mature macaques. *Nature.* 1996; 381:697–699. [PubMed: 8649514]
36. Constantinidis C, Steinmetz MA. Posterior parietal cortex automatically encodes the location of salient stimuli. *J Neurosci.* 2005; 25:233–238. [PubMed: 15634786]
37. Meyer T, Constantinidis C. A software solution for the control of visual behavioral experimentation. *J Neurosci Methods.* 2005; 142:27–34. [PubMed: 15652614]
38. Brainard DH. The Psychophysics Toolbox. *Spat Vis.* 1997; 10:433–436. [PubMed: 9176952]
39. Cavada C, Goldman-Rakic PS. Posterior parietal cortex in rhesus monkey: I. Parcellation of areas based on distinctive limbic and sensory corticocortical connections. *J Comp Neurol.* 1989; 287:393–421. [PubMed: 2477405]
40. Harris KD, Henze DA, Csicsvari J, Hirase H, Buzsaki G. Accuracy of tetrode spike separation as determined by simultaneous intracellular and extracellular measurements. *J Neurophysiol.* 2000; 84:401–414. [PubMed: 10899214]
41. White BJ, Munoz DP. Separate visual signals for saccade initiation during target selection in the primate superior colliculus. *J Neurosci.* 2011; 31:1570–1578. [PubMed: 21289164]
42. Davison, AC.; Hinkley, DV. *Bootstrap methods and their application.* Cambridge University Press; 1997.
43. Rowland BA, Quessy S, Stanford TR, Stein BE. Multisensory integration shortens physiological response latencies. *J Neurosci.* 2007; 27:5879–5884. [PubMed: 17537958]
44. Tolhurst DJ, Movshon JA, Dean AF. The statistical reliability of signals in single neurons in cat and monkey visual cortex. *Vision Res.* 1983; 23:775–785. [PubMed: 6623937]
45. Dayan, P.; Abbott, LF. *Theoretical Neuroscience. Computational and mathematical modeling of neural systems.* The MIT Press; 2001.

**Figure 1.**

Schematic diagram of the behavioral tasks and the monkey brain. **a.** Delayed match-to-sample task. The monkey was required to locate the salient stimulus in the cue frame and release a lever when a matching stimulus appeared. **b.** Schematic diagram of the monkey brain and areas where recordings were performed. Abbreviations: AS, arcuate sulcus; IPS, intraparietal sulcus; PS, principal sulcus; STS, superior temporal sulcus. **c.** Reaction-time version of the task. The monkey was required to release the lever immediately if a target was present and continue to hold it if it was absent.

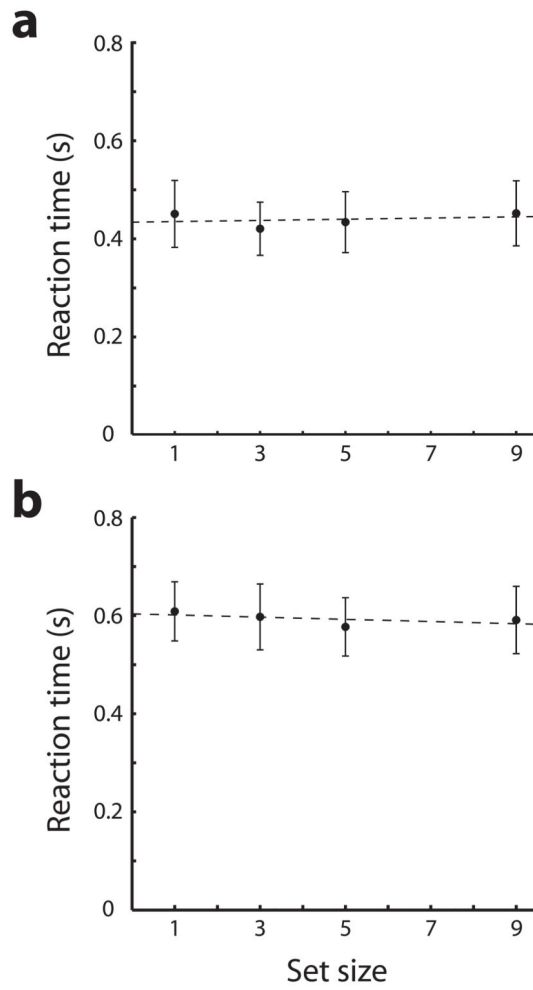


Figure 2. Behavioral response time as a function of stimulus set size. The reaction time version of the task was used. **a.** Average of 30 sessions is plotted for one monkey. **b.** Average of 13 sessions is plotted for the second monkey using the dense stimulus array. Error bars represent standard deviations across individual trials.

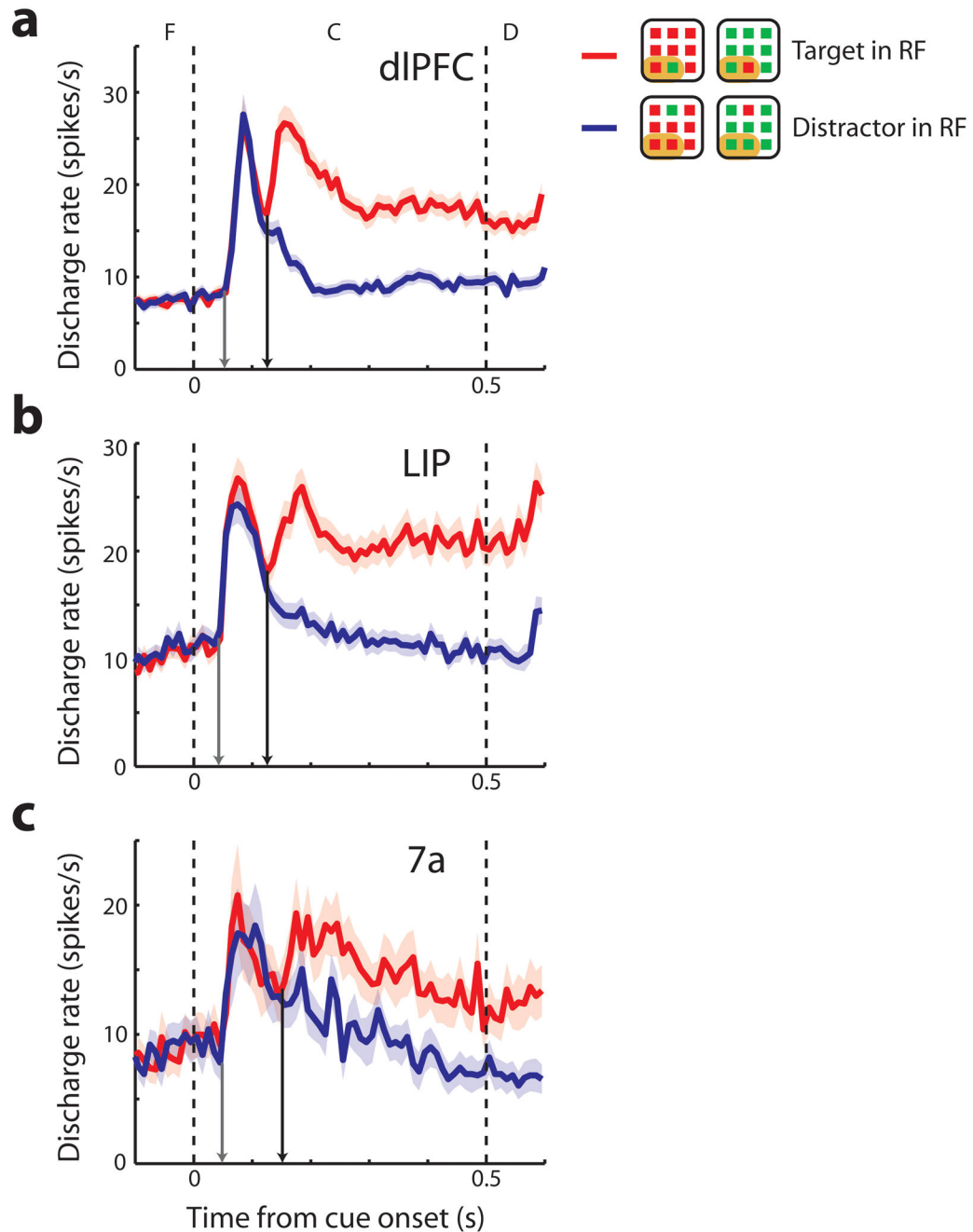


Figure 3.

Population firing rate. **a–c.** Average discharge rates from dIPFC (N=278), LIP (N=187), and area 7a (N=71) respectively. Peri stimulus time histograms are plotted with mean discharge rate elicited during presentation of target in the receptive field (RF) and distractor in the receptive field conditions over fixation (F), cue (C), and delay (D) period. Shaded area represents standard error of the mean discharge rate. The dotted vertical lines illustrate the time of cue onset and offset. Gray arrows in each panel indicate the population visual response latency; black arrows, the population time of neuronal target discrimination. Insets

are schematic illustrations of stimulus condition in or out of the receptive field; each neuron's receptive field was located at a different position.

Author Manuscript

Author Manuscript

Author Manuscript

Author Manuscript

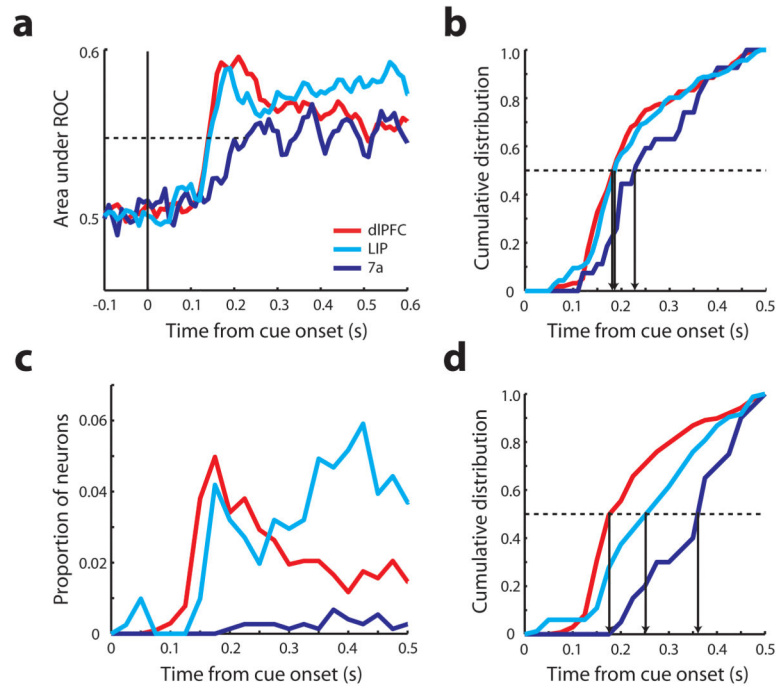


Figure 4.

Receiver operating characteristic (ROC) analysis and mutual information analysis. **a.** Area under the ROC curve is plotted as a function of time. Solid vertical line represents the time of cue onset. Dotted line indicates the average mid-point between the peak and baseline of recorded neurons irrespective of area. Red, cyan, and blue curves represent dIPFC (N=278), LIP (N=187), and area 7a (N=71) respectively. **b.** Cumulative distribution of neurons with significant area under the ROC curve. Each vertical arrow indicates the time point when 50% of neurons of an area reached significance (dIPFC: N=170, LIP: N=114, 7a: N=31). **c.** Proportion of neurons with significant mutual information as a function of time. Total sample size, dIPFC: N=793, LIP: N=406, 7a: N=485. **d.** Cumulative distribution of neurons that represented significant mutual information (dIPFC: N=137, LIP: N=83, 7a: N=20). Vertical arrow indicates the time point when 50% of neurons in an area reached statistical significance.

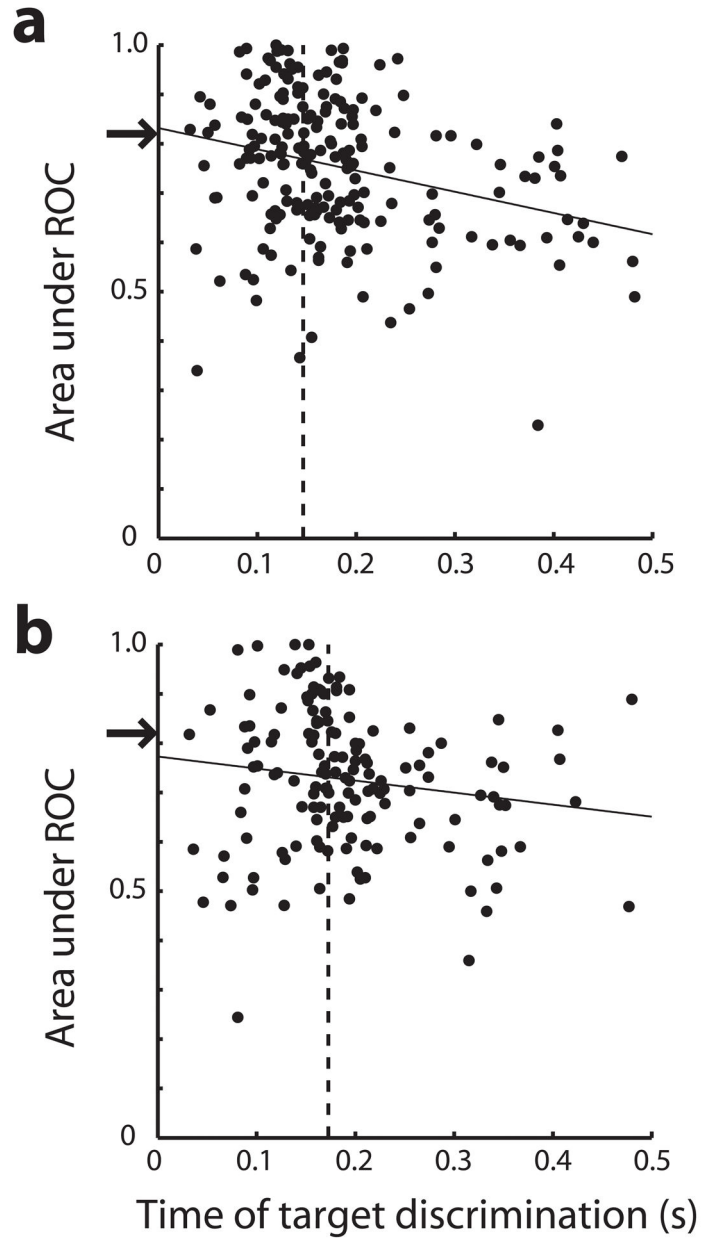


Figure 5. Relationship between discriminability and time of target discrimination. Area under the ROC curve over the entire stimulus presentation period (discriminability value) is plotted as a function of the time of target discrimination for each neuron for **a**, dIPFC **b**, LIP. Solid lines represent regression of area under the ROC curve on time of target discrimination. Arrows indicate the top quartile of ROC values obtained after pooling the values of both areas together; vertical dotted lines represent the mean time of target discrimination in each area based on neurons with ROC values above the arrow.

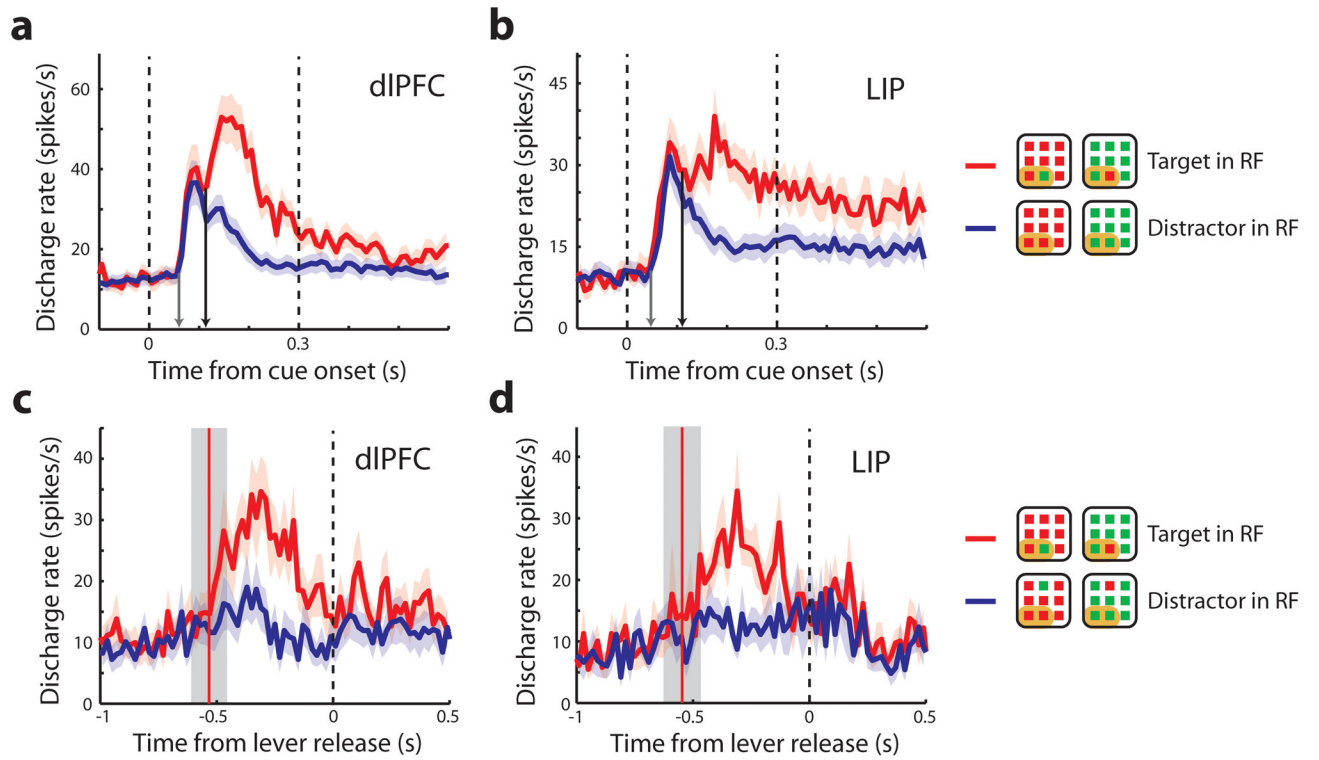
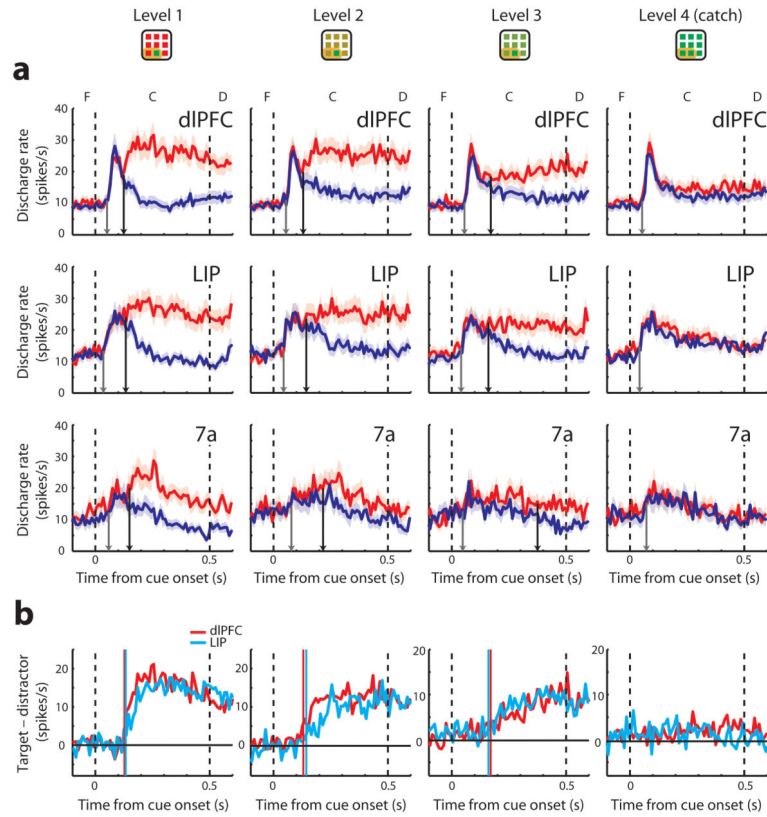


Figure 6.

Population responses during the reaction-time task. **a,b.** Mean discharge rate of target in the receptive field (RF) and distractor in the receptive field during fixation (F), cue (C), and delay (D) periods are plotted (dIPFC: N=42, LIP: N=36 neurons from one monkey). The arrows indicate the visual response latency (gray arrow) and the time of neuronal target discrimination (black arrow). **c,d.** Average discharge rate synchronized to lever release; only neurons recorded simultaneously are included here (dIPFC: N=17, LIP: N=9). Vertical red line and gray zone represents mean and 1 standard deviation around the time of stimulus presentation, relative to the response time.

**Figure 7.**

Population responses in the difficult-discrimination task. **a.** Responses of target in the receptive field (red lines) and distractor in the receptive field (blue lines) are plotted for the three brain areas at four levels of difficulty (dIPFC: N=58, LIP: N=55, area 7a: N=25). The arrows indicate the response onset latency (gray) and the time of neuronal target discrimination (black arrow). Data from salient stimuli of both colors have been pooled together (only one color is shown in the insets). **b.** Average difference in responses between a salient stimulus and a distractor in the difficult-discrimination task. Vertical lines represent time of target discrimination in dIPFC (red line) and LIP (cyan line).

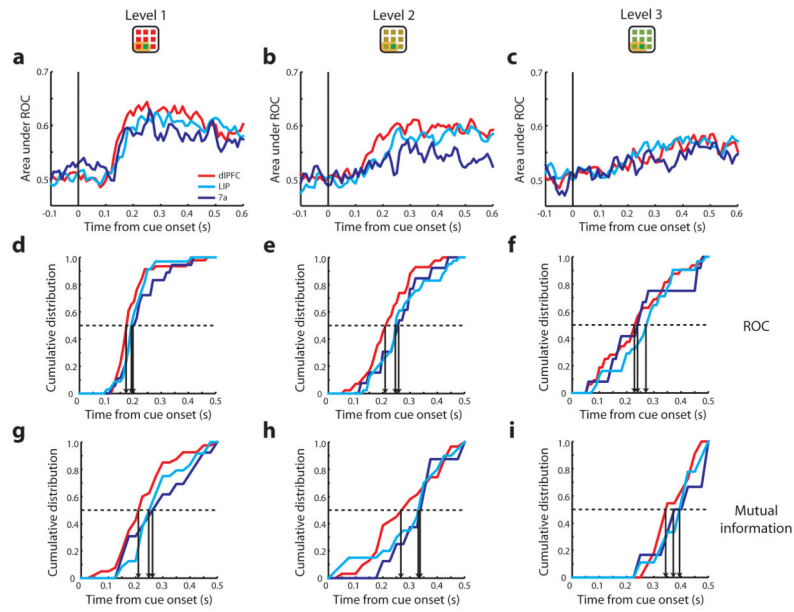


Figure 8. ROC and mutual information analysis for responses in the difficult-discrimination task. **a–c.** Average ROC values obtained from three levels of difficulty, respectively. Vertical lines illustrate the time of cue onset. **d–f.** Cumulative distribution of neurons with significant area under the ROC curve. **g–i.** Cumulative distribution of neurons that represented significant mutual information. Each vertical arrow indicates the time point when 50% of neurons in an area reached significance.